

# Intermolecular vibrational energy exchange directly probed with ultrafast two dimensional infrared spectroscopy

Hongtao Bian,<sup>1</sup> Wei Zhao,<sup>2</sup> and Junrong Zheng<sup>1,a)</sup>

<sup>1</sup>*Department of Chemistry, Rice University, Houston, Texas 77005, USA*

<sup>2</sup>*Department of Chemistry, University of Arkansas, Little Rock, Arkansas 72204, USA*

(Received 29 May 2009; accepted 5 August 2009; published online 22 September 2009)

Ultrafast two dimensional infrared (2D IR) spectroscopy has been applied to probe the intermolecular vibrational energy exchange between two model molecules, benzonitrile and acetonitrile- $d_3$ . The vibrational energy exchange between these two molecules is manifested through the growth of cross peaks in their 2D IR spectra. In experiments, their nitrile groups (CN) are not involved in the energy exchange but serve as reporters of the process. Our experiments demonstrate that intermolecular vibrational energy transfer can be directly probed with the 2D IR method. Results also show that the mode specific energy transfer can be important in intermolecular vibrational energy transfers. © 2009 American Institute of Physics. [doi:10.1063/1.3212618]

## I. INTRODUCTION

The intermolecular vibrational energy transfer is one of central issues in molecular dynamic studies. From small molecular chemical reactions to the conversion of chemical energy into mechanical energy in motor proteins, almost any chemical-bond-breaking or forming process requires the transfer of energy either into or out of a molecule's vibrational modes.<sup>1–11</sup> To understand and then learn to control the energy flow has long been a dream of physical chemists. During the past 80 years, a variety of techniques from ultrasonic absorption and dispersion to ultrafast lasers have been invented to investigate the vibrational energy transfer.<sup>5,12–15</sup> Among them, the ultrafast IR pump/probe and the ultrafast IR-pump/Raman-probe methods are the most widely used in these days.<sup>5,13–15</sup> In IR pump/probe measurements, the intermolecular vibrational energy transfer is indirectly obtained from vibrational relaxations<sup>16</sup> or anisotropy relaxations of the probe.<sup>17</sup> In IR-pump/Raman-probe measurements, the intermolecular vibrational energy transfer is directly monitored through the signal growth of energy-accepting vibrational modes in the Raman probe spectra.<sup>5</sup> Tremendous information about molecular vibrational energy transfer has been obtained with these methods.<sup>4,5,13,15,18–25</sup>

In this work, we will introduce another method which can directly probe the intermolecular vibrational energy transfer. Different from the IR-pump/Raman-probe technique, our method does not require the probe vibrational mode to be involved in the intermolecular energy transfer. The new method will be particularly useful in probing the energy exchange dynamics and molecular interaction details in complex systems, e.g., some biological molecules or relatively big molecules, where the energy exchanging modes overlap in frequencies. The method is based on the ultrafast two dimensional infrared (2D IR) techniques.

Ultrafast 2D IR spectroscopy is an ultrafast IR analog of

2D NMR that directly probes the structural degrees of freedom of molecules.<sup>26–58</sup> In a manner somewhat akin to NMR, the 2D IR technique involves a pulse sequence that induces and then probes the evolution of excitations (vibrations) of a molecular system. The 2D IR spectrum can also display intramolecular interactions and dynamics that are not observables in a linear IR vibrational absorption experiment. A critical difference between the 2D IR and NMR variants is that the IR pulse sequence is sensitive to dynamics on time scales 6–10 orders of magnitude faster than the NMR. Under developing for around ten years, the ultrafast 2D IR techniques have begun to gain applications in determining reaction mechanisms,<sup>29,31,44</sup> peptide and protein dynamics and structures,<sup>32,36,45,48,59–67</sup> charge transfer,<sup>53,68</sup> vibrational coupling and energy relaxations,<sup>50,51,69,70</sup> water structures and dynamics,<sup>47,72–77</sup> hydrogen bond kinetics and thermodynamics,<sup>28,39,56,58,78,79</sup> and chemical transformations.<sup>57</sup> To directly probe the intermolecular vibrational energy exchange introduced here is another application of the 2D IR technique.

## II. EXPERIMENTS

The 2D IR experimental setup is briefly described in the following. Three successive IR pulses ( $\sim 1 \mu\text{J}/\text{pulse}$ ) with the same polarization were applied to induce the subsequent emission in a distinct direction of a time delayed signal from both the rephasing phase match direction  $k_e = -k_1 + k_2 + k_3$  and the nonrephasing phase match direction  $k_{ne} = k_1 - k_2 + k_3$ . The transform-limited pulses ( $\sim 55 \text{ fs}$ ,  $\sim 4$  cycles of light) are produced using a Ti:sapphire regeneratively amplified laser system pumping an optical parametric amplifier. The IR pulses span sufficient bandwidth ( $300 \text{ cm}^{-1}$ ) with tunable central wavelength from 3 to  $10 \mu\text{m}$ . The vibrational echo pulse is detected with frequency and phase resolution by combining it with a fourth (local oscillator) pulse, and the combined pulses are dispersed in a spectrograph. The function of the local oscillator is to phase resolve and amplify the vibrational echo signal. Data are thus obtained as a function

<sup>a)</sup>Author to whom correspondence should be addressed. Electronic mail: junrong@rice.edu.

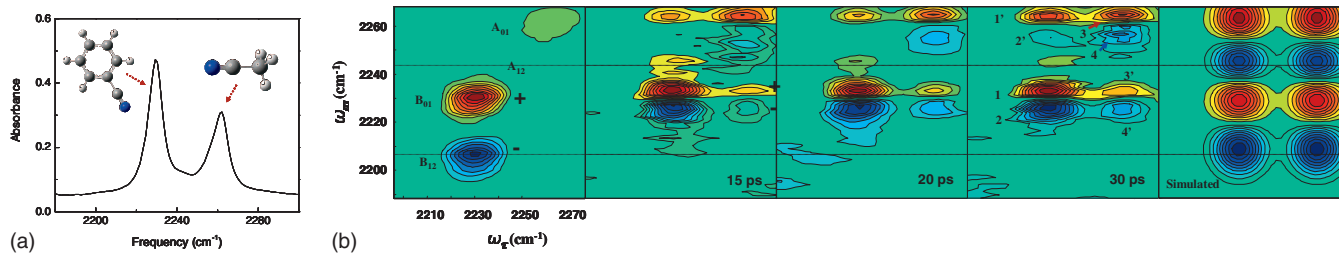


FIG. 1. FTIR and waiting time  $T_w$  dependent 2D IR spectra of CN groups of acetonitrile- $d_3$  ( $\sim 2263$   $\text{cm}^{-1}$ ) and benzonitrile ( $\sim 2230$   $\text{cm}^{-1}$ ) molecules in a mixed acetonitrile- $d_3$  (A) and benzonitrile (B) solution (molar ratio A/B  $\sim 1.8$ ) at room temperature. In the solution, after the CN stretches are excited to the first excited states, the vibrational energy of the nitrile groups of both molecules mostly relaxes intramolecularly to low frequency modes, and then the vibrational energy of some of the low frequency modes exchanges between the two molecules. The energy exchange is manifested by the growth of the cross peaks in 2D IR spectra. Note: very little vibrational energy has exchanged directly between the nitrile groups, since no 1-2 exchange cross peaks [should be at the positions of (2263  $\text{cm}^{-1}$ , 2208  $\text{cm}^{-1}$ ) and (2230  $\text{cm}^{-1}$ , 2245  $\text{cm}^{-1}$ )] have been observed. Each contour represents 10% amplitude increase [from  $-1$  (blue) to  $1$  (red)]. A simulated 2D IR spectrum for direct CN mode energy exchange is provided for comparison. The lines are drawn to aid determining the blue peak positions along the  $\omega_m$  axis.

of three variables: The emitted vibrational echo frequencies  $\omega_m$ , the variable time delays between the first and second pulses ( $\tau$ ), and second and third pulses ( $T_w$ , the variable “waiting” time). By numerical Fourier transform, the  $\tau$  scan data taken at every  $\omega_m$  are mapped to a second frequency variable  $\omega_\tau$  for each  $T_w$ . The echo and free induction decay data are then summed together with proper phase correlations to remove most of the dispersion contribution.<sup>34,80</sup> The data are then plotted in three dimensions, the amplitude as a function of both  $\omega_\tau$  and  $\omega_m$ , which correspond to the  $\omega_1$  and  $\omega_3$  axes, respectively, in 2D NMR. All the experiments were performed at room temperature.

The vibrational lifetimes and rotational relaxation times for the samples were measured with the polarization selective broadband IR pump-probe experiments. The laser source is the same as used for the 2D IR experiments. For the pump-probe experiments, the mid-IR pulse was spitted into two beams of intensity ratio 20:1. The beam with higher intensity served as the pump. The weaker one is the probe beam. The pump beam had horizontal polarization, while the probe beam polarization was  $45^\circ$  relative to the pump beam. The probe beam was passed through a spectrograph and detected by a 64-element HgCdTe array detector. A polarizer was placed in front of the spectrograph aligned to selectively measure the parallel or perpendicular polarized signal relative to the pump beam. Each polarized signal was normalized by the intensity of the probe beam with its polarization at the detector in the absence of the pump (the tail match method was also applied to make a comparison). The method eliminates possible sources of error such as phase shifts caused by mirrors and different diffraction efficiencies of the grating for different polarizations.

The chemicals benzonitrile,  $\text{CD}_3\text{CN}$ ,  $\text{CCl}_4$ , and  $\text{CHCl}_3$  were purchased from Aldrich and used as received. Temperature dependent Fourier transform infrared (FTIR) measurements were performed with a ThermoFisher FTIR spectrometer and a temperature controller from Harrick Scientific.

The structures were determined with density functional theory (DFT) calculations.<sup>81</sup> The DFT calculations were carried out as implemented in the GAUSSIAN 98 program suite. The level and basis set used were Becke’s three-parameter hybrid functional combined with the Lee–Yang–Parr correction functional, abbreviated as B3LYP, and 6-31+G( $d,p$ ).

All results reported here do not include the surrounding solvent and therefore are for the isolated molecules.

### III. RESULTS AND DISCUSSIONS

#### A. One dimensional and 2D IR spectra

Figure 1 shows the FTIR and waiting time  $T_w$  dependent 2D IR spectra of CN groups of acetonitrile- $d_3$  ( $\sim 2263$   $\text{cm}^{-1}$ ) and benzonitrile ( $\sim 2230$   $\text{cm}^{-1}$ ) molecules in a mixed acetonitrile- $d_3$  (A) and benzonitrile (B) solution (molar ratio A/B  $\sim 1.8$ ) at room temperature. In panel 2 ps, the red peak  $B_{01}$  at (2230  $\text{cm}^{-1}$ , 2230  $\text{cm}^{-1}$ ) belongs to the 0-1 transition and the blue peak  $B_{12}$  at (2230  $\text{cm}^{-1}$ , 2209  $\text{cm}^{-1}$ ) belongs to the 1-2 transition of the CN stretch of benzonitrile. The red peak  $A_{01}$  at (2263  $\text{cm}^{-1}$ , 2263  $\text{cm}^{-1}$ ) and the blue peak  $A_{12}$  at (2263  $\text{cm}^{-1}$ , 2245  $\text{cm}^{-1}$ ) belong to the CN stretch transitions of acetonitrile- $d_3$ . In the mixture, the two molecules are close to each other. It would be expected that the vibrational excitation of the CN stretch of one molecule can be transferred to the other in a relatively short period of time. The energy transfer dynamics can not be measured with FTIR, but it can be directly detected with the 2D IR method. The energy transfer dynamics is manifested by the growth of cross peaks in 2D IR spectra. As we can see from the 2D IR spectra, at a short time, there are only two diagonal red peaks and two corresponding blue peaks. With the increase in time, two salient changes appear in the 2D IR spectra. One is that two pairs of cross peaks grow in. The other is that the blue peaks shift to higher frequencies along  $\omega_m$ . As reported in literature, the growth of cross peaks in 2D IR spectra can come from chemical exchanges, vibrational couplings, and intramolecular vibrational energy transfer.<sup>27,33,37,57,58</sup> The cross peaks in Fig. 1 come from none of these. They are from the intermolecular vibrational energy exchange between  $\text{CD}_3\text{CN}$  and benzonitrile. The chemical nature of the system determines that this is the only possible mechanism for generating such cross peaks. Reasons are stated in the following. (1) In the mixture, the two molecules, benzonitrile and  $\text{CD}_3\text{CN}$ , can not ever chemically interconvert into each other under our experimental condition. Therefore, chemical exchange is not a possible reason for the growth of the cross peaks. (2) Intramolecular vibrational relaxation is not a cause

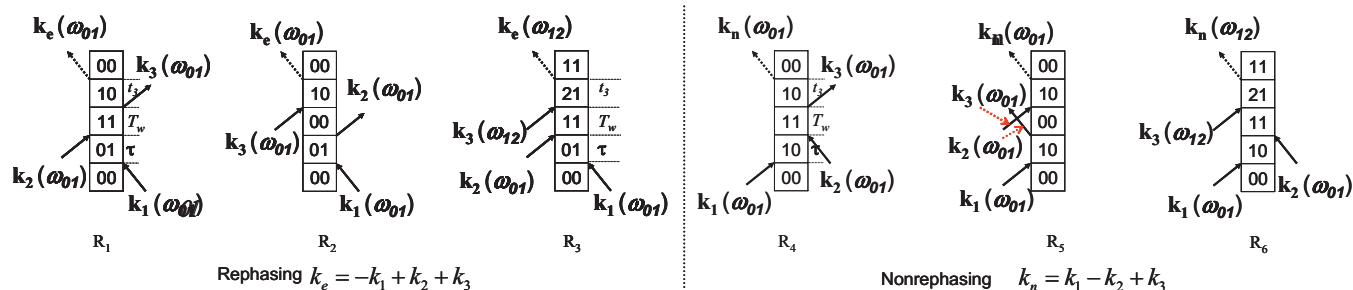


FIG. 2. Feynman diagrams contributing to peaks in Fig. 1 panel 2 ps. 0 represents the ground state and 1 represents the first excited states of the CN stretch mode. The 2D IR signal and the pump/probe signal (see below) are from both rephasing and nonrephasing pathways. Diagrams  $R_1$  and  $R_4$  are the first excited state stimulated emission. Diagrams  $R_2$  and  $R_5$  are the ground state bleaching. Diagrams  $R_3$  and  $R_6$  are the first excited state absorption. The frequencies  $\omega_\tau$  and  $\omega_m$  in 2D IR spectra are determined by the oscillating frequencies during the  $\tau$  and  $t_3$  periods, respectively.

too, since no experimentally observed modes other than the CN stretches in either molecule have vibrational frequencies at the region of  $2200\text{--}2270\text{ cm}^{-1}$  where the cross peaks appear. (3) Strong coupling will produce peaks at very short delay times, e.g., 100 fs. However, we do not see any cross peaks at 2 ps, which rules out this possibility. Now, one possibility remains. That is the intermolecular energy transfer, which has not been demonstrated in 2D IR before. In principle, there are two possible intermolecular energy transfers which can produce cross peaks. One is the direct energy transfer between the CN groups, and the other is the energy transfer between other modes which accepts energy relaxed from the CN groups intramolecularly. In the second possibility, the CN groups serve as the energy source and the reporter of the energy transfer because they are strongly coupled to the modes under intermolecular energy exchange. The strong coupling will produce combination band absorptions in 2D IR spectra, which can serve as the reporter of energy exchange. A detailed analysis is provided in next paragraphs.

It is relatively straightforward to distinguish these two intermolecular energy transfers from each other. Actually it is straightforward. If the transfer is between the CN groups, the exchange blue peaks 2' and 4' in panel 30 ps would be at the same positions as those CN 1-2 transition peaks  $A_{12}$  and  $B_{12}$  at 2 ps along the  $\omega_m$  axis, as shown in the simulated figure in Fig. 1. If transfer occurs among other modes, the exchange blue peaks will appear in the positions of the combination band absorption peaks 2 and 4 in panel 30 ps along the  $\omega_m$  axis, which is the case in experiments. The cross peaks grow with the reaction time, indicating how the energy is transferring. The detailed growth mechanism of the peaks is stated in the following.

In the 2D IR spectrum at 2 ps, the red contours are positive going (0-1 vibrational transition) and the blue contours are negative going (1-2 vibrational transition). As discussed further below, the 0-1 signal comes from two quantum pathways that are related to bleaching of the ground state and stimulated emission, both of which produce a signal that is in phase with and therefore adds to the local oscillator pulse to produce a positive going signal. The 1-2 signal arises because there is a new absorption that was not present prior to the first two excitation pulses. The 1-2 vibrational signal is  $180^\circ$  out of phase with and thus subtracts

from the local oscillator to produce a negative going signal. At  $T_w=2$  ps, there are two peaks on the diagonal (0-1 transitions) and the corresponding 1-2 transition peaks off-diagonal. There are no off-diagonal peaks in the 0-1 region because 2 ps is short compared to the exchange time.  $T_w=30$  ps is long compared to the exchange time, and additional peaks have grown in.

Peak origins in 2D IR spectra can be interpreted with the diagrammatic perturbation theory.<sup>41,82</sup> Here a brief qualitative description will be given. Detailed diagrams showing how all the peaks are generated are in Figs. 2 and 5. The frequency at which the first pulse excites a mode is the mode frequency on the  $\omega_\tau$  axis (horizontal axis),  $2263\text{ cm}^{-1}$  for the CN 0-1 transition of acetonitrile- $d_3$  and  $2230\text{ cm}^{-1}$  for benzonitrile. The third pulse causes a mode to emit the time delayed signal at the same frequency as the vibrational mode that interacted with the third pulse. The frequency of the signal emission is the frequency on the  $\omega_m$  axis (the vertical axis). First consider the 2D IR spectrum panel 2 ps in which the data are taken prior to energy exchange. For the 0-1 vibrational transitions, the third pulse induces the signal at the same frequencies excited by the first pulse, so there are two peaks on the diagonal where  $\omega_\tau=\omega_m$  [red peaks (+) in panel 2 ps]. If the signal frequency ( $\omega_m$ , third pulse frequency) is different from the frequency of initial excitation ( $\omega_\tau$ , first pulse frequency), peaks will appear off-diagonal. Again, in panel 2 ps, the blue peaks are off-diagonal by the vibrational anharmonicity because the modes are initially excited at their 0-1 frequencies ( $\omega_\tau$ ) but the third pulse causes vibrational echo emission at their 1-2 frequencies ( $\omega_m$ ).

Figure 2 displays the Feynman diagrams of peak origins in panel 2 ps in Fig. 1. In the diagrams, 0 represents the ground state (in theory, 0 is an index of the density matrix), 1 represents the first excited states of the CN stretch mode. The 2D IR signal and the pump/probe signal (see below) are from both rephasing and nonrephasing pathways. Diagrams  $R_1$  and  $R_4$  are the first excited state stimulated emission. Diagrams  $R_2$  and  $R_5$  are the ground state bleaching. Diagrams  $R_3$  and  $R_6$  are the first excited state absorption. The frequencies  $\omega_\tau$  and  $\omega_m$  in 2D IR spectra are determined by the oscillating frequencies during the  $\tau$  and  $t_3$  periods, respectively. The frequency in the  $\tau$  period for all six diagrams is  $\omega_{01}$  (for A,  $\omega_{01}=2263\text{ cm}^{-1}$ ; for B,  $\omega_{01}=2230\text{ cm}^{-1}$ ). The  $t_3$  frequency for the ground state bleaching and the stimu-

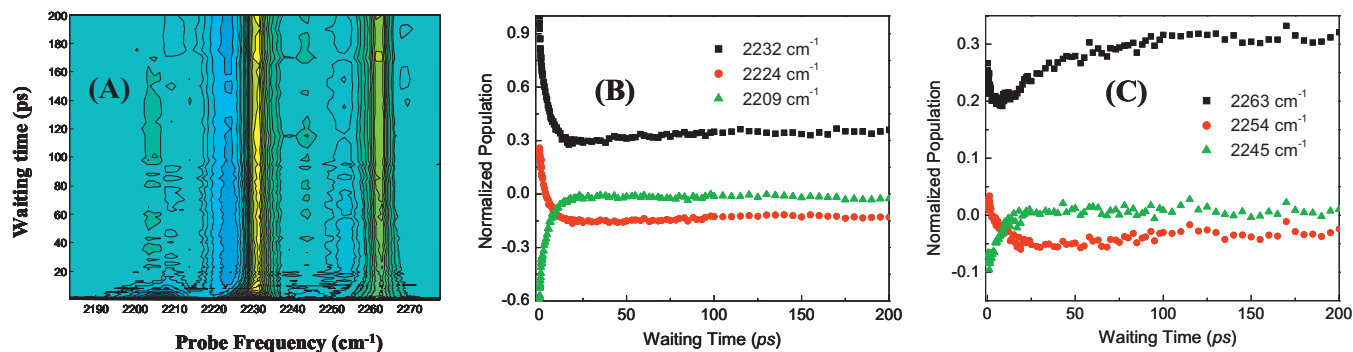


FIG. 3. Rotation-free pump/probe spectra and data of the  $\text{CD}_3\text{CN}$ /benzonitrile mixture. (a) Broad band pump/probe spectra. The small peak in (a) at  $2215\text{ cm}^{-1}$  and the dip at  $2210\text{ cm}^{-1}$  are assigned to an overtone of  $\text{CD}_3\text{CN}$ . The small peak at  $2204\text{ cm}^{-1}$  is assigned to an overtone of benzonitrile. The peak at  $2245\text{ cm}^{-1}$  is from another overtone of benzonitrile. All the assignments are based on FTIR measurements in both bulk samples and dilute  $\text{CCl}_4$  solutions. (b) and (c) are rotation free ( $I_{\parallel}+2I_{\perp}$ ) pump/probe data at the frequencies of CN 0-1 ( $2263$  and  $2230\text{ cm}^{-1}$ ) and 1-2 transitions ( $2209$  and  $2245\text{ cm}^{-1}$ ) and the CN/L ( $2224\text{ cm}^{-1}$ ) and L' ( $2254\text{ cm}^{-1}$ ) combination bands (see text for details). The CN vibrational lifetimes of benzonitrile and  $\text{CD}_3\text{CN}$  are determined to be  $T_B=4.2\text{ ps}$  and  $T_A=9.0\text{ ps}$ , respectively, from single exponential fitting to the 1-2 transition signal decays.

lated emission diagrams is also  $\omega_{01}$ , resulting in diagonal peaks  $A_{01}$  and  $B_{01}$  ( $\omega_{\tau}=\omega_m=\omega_{01}$ ) in panel 2 ps. The  $t_3$  frequency for the first excited state absorption diagrams is  $\omega_{12}$  (for A,  $\omega_{12}=2245\text{ cm}^{-1}$ ; for B,  $\omega_{12}=2209\text{ cm}^{-1}$ ), resulting in off-diagonal peaks  $A_{12}$  and  $B_{12}$  ( $\omega_{\tau}=\omega_{01}$ ;  $\omega_m=\omega_{12}$ ).

The influence of intermolecular energy exchange on the 2D spectra can be easily understood in terms of the ideas presented above. If during the  $T_w$  period, the vibrational energy of some benzonitrile molecules transfers to some acetonitrile- $d_3$  molecules, then the third pulse will cause the emission of the signal at the frequency of the acetonitrile- $d_3$ . The frequency of emission  $\omega_m$  then differs from the excitation frequency  $\omega_{\tau}$  for these specific molecules. The result will be an off-diagonal peak that only appears if energy transfer occurs. Because the acetonitrile- $d_3$  absorbs at higher frequency than benzonitrile, this off-diagonal peak is shifted to higher frequency along the  $\omega_m$  axis by the frequency difference ( $33\text{ cm}^{-1}$ ) between the two molecules. Conversely, if during the  $T_w$  period, energy transfers from acetonitrile- $d_3$  to benzonitrile, then the third pulse will produce an off-diagonal peak shifted to lower frequency along the  $\omega_m$  axis by the same amount. Identical considerations apply for both the 0-1 and 1-2 regions of the spectrum. This behavior is shown in panel 30 ps in Fig. 1, wherein substantial energy exchange has led to the generation of four red peaks and four blue peaks; the two new pairs of peaks were not present at  $T_w=2\text{ ps}$ . Clearly vibrational energy has transferred between the two molecules. The growth of the additional off-diagonal peaks with increasing  $T_w$  is directly related to the time dependence of the intermolecular vibrational energy exchange.

The above explanation for energy exchange is similar to that for chemical exchanges.<sup>58</sup> However, intermolecular energy transfers are more complicated than chemical exchanges. The vibrational energy of one mode can transfer to other modes intramolecularly and intermolecularly simultaneously. This creates two possible intermolecular energy transfers in the system we studied: One is that energy directly transfers between CN groups of the two molecules; the other is that energy transfer is among mode(s) which accept(s) energy relaxed from the CN excitations. How can we distinguish these two mechanisms? We will combine pump/probe and 2D IR data to address this issue.

Figure 3 displays the rotation-free pump/probe spectra and waiting time dependent signal changes at some important probe frequencies of the  $\text{CD}_3\text{CN}$ /benzonitrile mixture. The vibrational lifetimes of the CN excitations can be obtained from the CN 1-2 transition signal decays at probe frequency of  $2245$  (for molecule A) and  $2209\text{ cm}^{-1}$  (for B), since the 1-2 signals are purely from the CN first excited state populations. Other time constants can also be obtained from the pump/probe data. See supporting materials<sup>83</sup> for details. Analyzing the data with single exponential decays yields the CN vibrational lifetime of benzonitrile to be  $T_B=4.2\text{ ps}$  and  $T_A=9.0\text{ ps}$  for  $\text{CD}_3\text{CN}$ . Such short vibrational lifetimes mean that most of the CN excitations will relax into other modes within 30 ps. Therefore, it is not likely that substantial vibrational populations initially excited can exchange between the two CN modes at  $T_w=30\text{ ps}$ . This indicates that the exchange cross peaks in the 2D IR spectra in Fig. 1 are not from the direct CN mode energy transfer, but from energy exchange among modes which accept energy relaxed from the CN modes. Another evidence to support this argument is the position of the exchange cross blue (–) peaks. In panel 15–30 ps, the blue peaks are at higher frequencies along the  $\omega_m$  axis than those corresponding CN 1-2 transition peaks in panel 2 ps. The position shifts are caused by the intramolecular energy relaxation, which has been observed in other systems.<sup>16,24,57,84,85</sup> If the cross peaks are caused by the direct energy exchange between the CN groups, the exchange blue peaks would be at the same positions along the  $\omega_m$  axis as those CN 1-2 transition peaks, similar to what happens in regular chemical exchange 2D IR spectra.<sup>58</sup> A simulated 2D IR spectrum from assumed direct energy exchange between the CN groups is displayed in Fig. 1 for comparison.

Now, another question arises. How does the intramolecular energy relaxation change the positions of the blue (–) peaks? Before answering this question, we construct a physical picture to describe what happens after the CN stretch modes are excited to their first excited state, shown in Fig. 4. In the picture, the populations on the CN first excited states begin to intramolecularly relax into other modes of low frequencies sooner after they are excited. Some of the low frequency modes, called **L** for A molecules and **L'** for B mol-

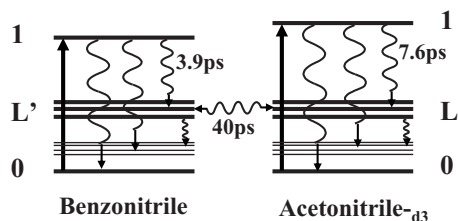


FIG. 4. Diagram describing how the intermolecular and intramolecular energy transfers proceed after the CN groups are excited in the mixed benzonitrile and acetonitrile- $d_3$  sample. After excited, the populations on the CN first excited states begin to intramolecularly relax into other modes at low frequencies and back to the ground states. Some of the low frequency modes, called  $L$  for A molecules and  $L'$  for B molecules, which are strongly coupled to the CN stretches, will then exchange energy between the two molecules. Finally, all the excitations will relax back to the ground states. The time constants are from experiments.

ecules, which are strongly coupled to the CN stretches, will then exchange energy between the two molecules. Finally, all the excitations will relax back to ground states. During the intramolecular relaxations, the excitations of  $L$  and  $L'$  create a phenomenon called combination band absorption:<sup>16,33</sup> both  $L$  (or  $L'$ ) and CN are excited. The combination band absorptions in both molecules generate blue (–) peaks 2 and 4 in the 2D IR spectra at frequencies higher than the corresponding CN 1-2 transition frequencies but lower than the 0-1 transitions along the  $\omega_m$  axis because of the anharmonic coupling between  $L$  (or  $L'$ ) and CN. In addition, the anharmonicity of the coupling between  $L$  (or  $L'$ ) and CN is smaller than the anharmonicity between the CN 0-1 and 1-2 transition. The anharmonicities can be directly obtained from the position difference along the  $\omega_m$  axis between the positive and negative peak pairs in 2D IR spectra, e.g., the CN 0-1 and 1-2 transition anharmonicity in benzonitrile is  $2230\text{ cm}^{-1} - 2209\text{ cm}^{-1} = 21\text{ cm}^{-1}$ . A more rigorous description about the peak frequency shifts and appearances of peaks after the intramolecular vibrational relaxations is provided in the following.

According to the physical picture described above and the pump/probe measurements, very few CN first excited state populations remain after 30 ps. Therefore, in panel 30 ps in Fig. 1, there is very little contribution from the first excited state stimulated emission to the diagonal red peak 1 or 3 any more, since most of the first excited state popula-

tions have relaxed away. The two peaks are purely from the ground state bleaching. There are two sources for the ground state bleaching. One is that the relaxation of the first excited state to some low frequency modes does not recover the ground state. The other is that the relaxed vibrational energy locally heats the molecules and makes the sample more transparent (mainly because of the absorption coefficient decrease caused by the temperature change, see temperature dependent data in supplementary material<sup>83</sup>). These two sources can both be represented by diagrams  $R_2$  and  $R_5$ . Blue peaks 2 and 4 are not CN's 1-2 transitions. They are combination band absorptions. The corresponding diagrams  $R_7$  and  $R_{10}$  for these two peaks are shown in Fig. 5. Cross peaks  $1' \sim 4'$  are from the energy exchange between the two molecules. Their origins can be represented with diagrams  $R_8$ ,  $R_9$ ,  $R_{11}$ , and  $R_{12}$  in Fig. 5.

Figure 5 displays the Feynman diagrams contributing to peaks in Fig. 1 panel 30 ps. 0 and 0' represent the ground state, 1 and 1' represent the first excited states of the CN stretch modes, and  $L$  and  $L'$  represent the low frequency modes of molecules A and B. The 2D IR signal and the pump/probe signal are from both rephasing and nonrephasing pathways. Diagrams  $R_7$  and  $R_{10}$  are the combination band absorption for peaks 2 and 4. In the diagrams, the oscillating frequency in the  $\tau$  period is  $\omega_\tau = \omega_{01}$  (for A,  $\omega_{01} = 2263\text{ cm}^{-1}$ ; for B,  $\omega_{01} = 2230\text{ cm}^{-1}$ ). During the population period  $T_w$ , the CN first excited state population 11 relaxes to low frequency mode(s)  $LL$ , resulting in the combination band absorption coherence in the  $t_3$  period with frequency  $\omega_m = \omega_{L-1+L}$  (for A,  $\omega_{L-1+L} = 2254\text{ cm}^{-1}$ ; for B,  $\omega_{L-1+L} = 2224\text{ cm}^{-1}$ ). Diagrams  $R_8$  and  $R_{11}$  are for the energy exchange ground state bleaching peaks 1' and 3'. The energy exchange of  $L$  and  $L'$  and heat, defined as populations of lower frequency modes which can not produce combination band absorptions with the CN groups but can change the cross sections of the CN absorptions, between the two molecules results in the exchange of ground state bleaching. In the two diagrams, the oscillating frequency in the  $\tau$  period is  $\omega_\tau = \omega_{01}$  (for A,  $\omega_{01} = 2263\text{ cm}^{-1}$ ; for B,  $\omega_{01} = 2230\text{ cm}^{-1}$ ), representing the origins of energy. During the population period  $T_w$ , the populations of  $L$  and  $L'$  and heat are under exchange between the two molecules. The exchanges create ground state population holes on the energy

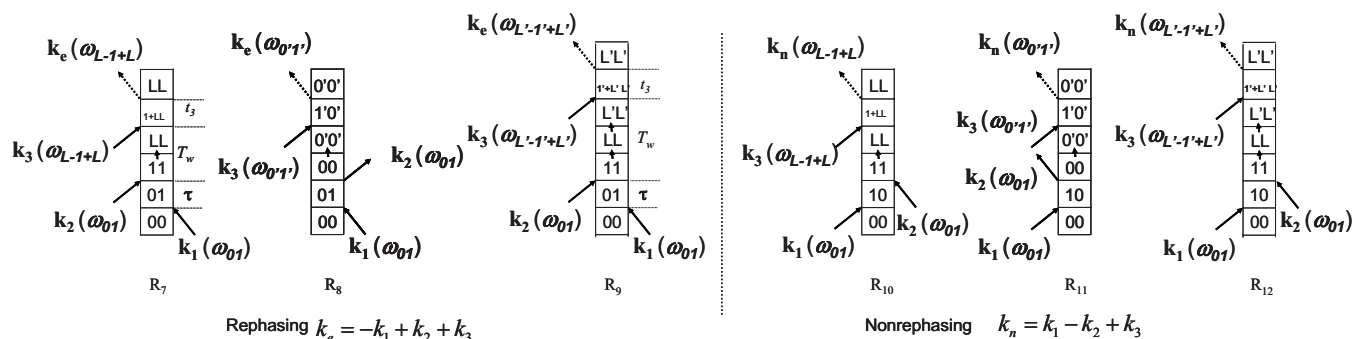


FIG. 5. Feynman diagrams contributing to peaks in Fig. 1 panel 30 ps. 0 and 0' represent the ground state, 1 and 1' represent the first excited states of the CN stretch modes, and  $L$  and  $L'$  represent the low frequency modes of molecules A and B. The 2D IR signal and the pump/probe signal (see below) are from both rephasing and nonrephasing pathways. Diagrams  $R_7$  and  $R_{10}$  are the combination band absorption for peaks 2 and 4. Diagrams  $R_8$  and  $R_{11}$  are for the energy exchange ground state bleaching peaks 1' and 3'. Diagrams  $R_9$  and  $R_{12}$  are for the energy exchange combination band absorption peaks 2' and 4'.

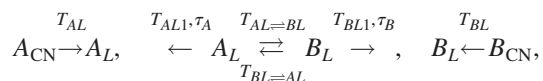


bands or overtones with very low IR intensities are not considered, then the most likely  $L$  and  $L'$  would be the ring breathing motion of benzonitrile and the C–D bending of  $\text{CD}_3\text{CN}$  at  $\sim 1030\text{ cm}^{-1}$ .

One question will arise naturally. Why is there no vibrational energy exchange between the two CN groups observed while energy can effectively transfer between  $L$  and  $L'$ ? There are a few reasons. The first one is that the intramolecular vibrational energy relaxations of the CN stretches are much faster than the exchange between them because of stronger intramolecular couplings. No cross peaks at 2 ps in Fig. 1 indicates that the intermolecular coupling between the two CN groups is weak. Second, the vibrational lifetimes of  $L$  and  $L'$  are much longer [see pump/probe data at probe frequencies of  $2254$  and  $2224\text{ cm}^{-1}$  in Figs. 3(b) and 3(c)] than those of CN stretches. More importantly, the energy mismatches of  $L$  and  $L'$  between the two molecules are probably smaller than the frequency difference between the two CN groups, which allows the quasisonance or resonance energy transfer. In addition, molecular frictions also favor the low frequency energy transfer.<sup>12</sup> However, we can not draw a conclusion that the energy exchange between  $L$  and  $L'$  is more efficient than between the CN groups, since the short lifetimes of CN groups limit the observation of the direct energy exchange between them.

## B. Dynamics analysis

At a glance of the relative amplitudes of cross peaks in Fig. 1, we know that the intermolecular energy transfer between the two molecules occurs within tens of picoseconds. To more quantitatively analyze the energy transfer kinetics, several molecular dynamic processes need to be considered. First, the CN excitations intramolecularly relax to low frequency modes with time constants  $T_A=9.0\text{ ps}$  and  $T_B=4.2\text{ ps}$  (for molecules A and B, respectively). Second, parts of the CN excitations relax to the mode(s)  $L$  and  $L'$  which can generate combination absorption peaks 2 and 4 with time constants  $T_{AL}=7.6\text{ ps}$  and  $T_{BL}=3.9\text{ ps}$ , and then the excitations of the mode(s)  $L$  and  $L'$  exchange between molecules A and B with a time constant  $T_{AL=BL}$  (assume that the difference of mode(s)' frequencies between A and B is very small so that  $T_{AL=BL}=T_{BL=AL}$ ), while they also intramolecularly relax to lower frequency modes with time constants  $T_{AL1}=31\text{ ps}$  and  $T_{BL1}=80\text{ ps}$ . (These are apparent values from pump/probe data. The actual values are possibly bigger.) Third, the rest of the CN excitations relax to low frequency modes and finally into phonon modes ( $<500\text{ cm}^{-1}$ ), the excitations of these modes can also exchange between A and B with a time constant  $T_{AP=BP}$ . Forth, the 2D IR signal is also affected by the molecular rotations, which make all peaks decay. The rotational time constants are  $\tau_A=2\text{ ps}$  and  $\tau_B=5.3\text{ ps}$ . The kinetic model to analyze  $T_{AL=BL}$  is therefore constructed, as shown in the following scheme:



where  $A_{\text{CN}}$  and  $B_{\text{CN}}$  are the populations of CN first excited states.  $A_L$  and  $B_L$  are the populations of  $L$  and  $L'$  first excited

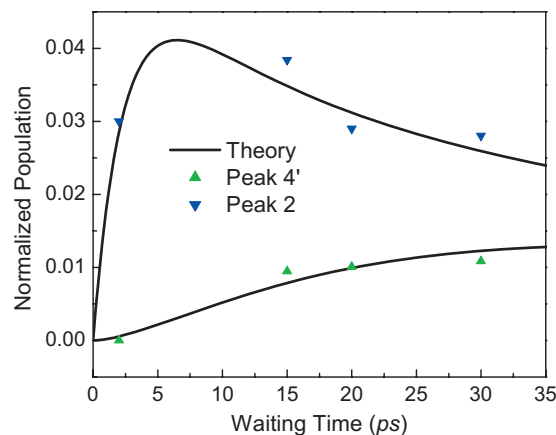


FIG. 7. Data and kinetic model calculations to yield the energy exchange time constant  $T_{AL=BL}=50\text{ ps}$ . Dots are normalized excited populations of  $L'$  of B from peaks 2 and 4' in Fig. 1. Lines are calculated results. Input parameters (experimentally measured) into calculations are  $T_{AL}=8.1\text{ ps}$ ,  $T_{BL}=3.9\text{ ps}$ ,  $\tau_A=2\text{ ps}$  and  $\tau_B=5.3\text{ ps}$ ,  $T_{AL1}=90\text{ ps}$ ,  $T_{BL1}=160\text{ ps}$ .  $T_{AL1}$  and  $T_{BL1}$  are allowed to vary in the calculations. In calculations, the energy exchange is assumed to be resonant. The initial relative excited state populations of CNs are determined with FTIR to be 0.58(B):0.42(A), and the transition dipole moment square ratio (B/A) is determined to be 2.5. Only 20% of the initial CN stretch energy of A and 15% of that of B are relaxed to  $L$ s, determined from pump/probe measurements. We assume that all energy of  $L$  and  $L'$  measured from the combination peaks can exchange.

states, respectively. In the model, all the populations can be obtained from 2D IR measurements, and the time constants were obtained from pump/probe measurements. The only unknown parameter  $T_{AL=BL}$  can be derived from the model with already known experimental parameters. To analytically solve this model, the CN relaxations to  $L$  or  $L'$  are assumed to be much faster than the energy exchange between A and B, and therefore can be decoupled from the exchange processing. The analytical solution for the energy exchange is then identical to what was for the chemical exchange model.<sup>58,78</sup>

As analyzed above, the red peaks at longer waiting times  $T_w$  in Fig. 1 contain contributions from both  $L$  and  $L'$  and heat, while blue peaks 2, 2', 4', and 4 are mainly from  $L$  and  $L'$ . Peaks 2' and 4 overlap with some red peaks. We therefore only pick up peaks 2 and 4' to analyze the energy exchange kinetics. Theoretical fits to the model with experimental data yield the only parameter  $T_{AL=BL}=30\text{ ps}$ . The fits do not reproduce peak 2 very well, which is probably because the relaxation time constants of  $L$  and  $L'$  can not be precisely measured. They are derived from signal changes, which are also caused by the energy exchange. Therefore, the two time constants  $T_{AL1}$  and  $T_{BL1}$  are allowed to vary in another fit, which yields  $T_{AL=BL}=50\text{ ps}$ . From the two fits, we conclude that the vibrational energy of mode(s)  $L$  between  $\text{CD}_3\text{CN}$  and benzonitrile exchanges with a time constant  $T_{AL=BL}=40 \pm 10\text{ ps}$ . Results are displayed in Fig. 7. Because many dynamic processes are coupled together in the system and  $L$  and  $L'$  are not single modes, the analysis here can be only considered as semiquantitative.

## C. Heating effect

In the system studied, the vibrational energy of CN will eventually change into thermal energy and locally heat up

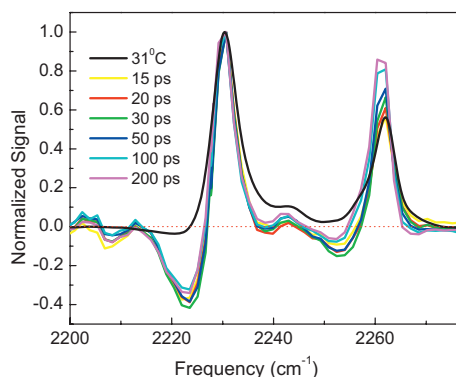


FIG. 8. Temperature dependent IR spectral difference between 54 and 23 °C (black line 31 °C) and pump/probe spectra at different time delays. The spectral difference is obtained from  $(\text{transmittance}_{54\text{ }^\circ\text{C}} - \text{transmittance}_{23\text{ }^\circ\text{C}}) / \text{transmittance}_{23\text{ }^\circ\text{C}}$  in linear IR measurements. The data clearly show that the dip at 2224  $\text{cm}^{-1}$  (the sum of peaks 2 and 4' in Fig. 1) is not from heating.

the molecules. Heat from vibrational relaxations can possibly shift the vibrational frequencies and therefore produces new peaks in 2D IR spectra.<sup>54,88,89</sup> As mentioned above, red peaks in panels 20 and 30 ps in Fig. 1 partially come from heating, while the contribution of heating to the blue peaks is relatively small. This claim can be directly confirmed with temperature dependent FTIR spectra and pump/probe measurements. The comparison between FTIR difference spectrum and pump/probe data is similar to what was done in literature.<sup>88</sup>

Figure 8 displays temperature-different (54–23 °C) IR spectrum and pump/probe spectra at different delays of the  $\text{CD}_3\text{CN}/\text{benzonitrile}$  mixture. The temperature increase induces spectral bleaching in both CN 0-1 transitions and a tiny absorption (less than 5% of the bleaching) at the frequency of the combination band CN/ $L$  transition (2224  $\text{cm}^{-1}$ ) of benzonitrile. Combining the pump/probe signal decays in Figs. 3(b) and 3(c), we can estimate the heat generated after 200 ps delay. The pump/probe data [triangle curves in Figs. 3(b) and 3(c)] show that after 20 ps, most of the CN excitations have relaxed to other modes. Comparing the amplitudes of the combination signals [dot curves in Figs. 3(b) and 3(c)] at long delay times (e.g., 30 ps) to the original CN 0-1 transition signals [square curves in Figs. 3(b) and 3(c)] at very short delay times (e.g., 250 fs), we can find that  $\sim 20\%$  of the CN excitation of molecule A has relaxed to mode(s)  $L'$ , and  $\sim 15\%$  has relaxed to  $L$  in B. The amplitude ratio can directly represent the population ratio of  $L/\text{CN}$  because the combination absorption transition dipole moment is determined to be almost identical to the CN 0-1 transition based on pump/probe measurements in dilute solutions. Heating contributes to more than 50% of the CN 0-1 transition signals after 20 ps, determined from comparing the amplitudes of the combination signals to CN 0-1 transition signals. Only about 5% of the intensities of the combination band peaks in Fig. 1 are from heating, estimated from the absorption/bleaching ratio of the FTIR temperature difference spectra and pump/probe data. The temperature increase from 20 to 200 ps is only 1–2 K, obtained from comparing the pump/probe data and temperature dependent FTIR spectra (in supporting materials<sup>83</sup>).

An interesting feature in the pump/probe data is that the CN 0-1 transition signals increase after  $\sim 20$  ps. The increase amplitude (12% absolute value increase) of molecule A (2263  $\text{cm}^{-1}$ ) in Fig. 5(d) is bigger than molecule B [6% increase in Fig. 5(c)]. Combined with the 2D IR data, a reasonable explanation can be provided for the increase and the amplitude difference. The CN 0-1 transition pump/probe signals (after CN excitations have relaxed) at 2263 and 2230  $\text{cm}^{-1}$  in Fig. 3 are the sums of the red peaks 1' and 3 and 1 and 3' in Fig. 1 along  $\omega_\tau$ , respectively. Each pump/probe signal includes one diagonal and one cross red peaks, and it can be expressed as

$$I_A = c_{BL \rightarrow AL} \mu_A^2 \mu_B^2 + k_A c_{BH \rightarrow AH} \mu_A^2 + k_A (c_{AH} - c_{AH \rightarrow BH}) \mu_A^2 + (c_{AL} - c_{AL \rightarrow BL}) \mu_A^4,$$

$$I_B = c_{AL \rightarrow BL} \mu_A^2 \mu_B^2 + k_B c_{AH \rightarrow BH} \mu_B^2 + k_B (c_{BH} - c_{BH \rightarrow AH}) \mu_B^2 + (c_{BL} - c_{BL \rightarrow AL}) \mu_B^4, \quad (1)$$

where  $I_i$  is the signal of molecule  $i$ ,  $\mu_i$  is the transition dipole moment,  $c_{iL \rightarrow jL}$  is the population of mode(s)  $L$  transferred from  $i$  to  $j$ ,  $c_{iH \rightarrow jH}$  is the heat population transferred from  $i$  to  $j$ ,  $k_i$  is the spectral heat response, and  $c_{iH}$  and  $c_{iL}$  are the heat and  $L$  populations, respectively. All the populations are proportional to the initial energy deposited to the molecules ( $E_A/E_B = 0.42/0.58$ ). The transition dipole moment ratio is  $\mu_A/\mu_B = \sqrt{1}/2.5$ . The two ratios were from FTIR and laser spectrum measurements. The heat response ratio of A over B is 0.6, measured with temperature dependent FTIR. From Eq. (1), we can see that intramolecular energy relaxation into heat increases both  $I_A$  and  $I_B$ . However, the intermolecular energy transfer causes  $I_A$  to increase while  $I_B$  to decrease. The square curves in Figs. 3(b) and 3(c) are the results of these two effects.

The vibrational lifetimes of  $L$  and  $L'$  are relatively long, as we can see from the pump/probe spectra in Fig. 3. Such long vibrational lifetimes make sure that most of their excitations, which is 15%–20% of the initial CN excitation energy, can be transferred between molecules A and B.

#### D. Advantages and disadvantages

The popular method to study intermolecular vibrational energy transfer is IR pump/Raman probe.<sup>4,23</sup> In the method, the energy transfer is directly probed by observing the signal growth of the mode which accepts energy. The method is extremely powerful in finding the energy relaxation pathways. However, it is difficult to probe intermolecular resonance vibrational transfer, since it is almost impossible to distinguish the identities of modes under energy exchange if the modes are on resonance. The resonance vibrational energy transfer can be probed through anisotropy changes with the IR pump/probe method. In the method, the exchanging modes need to be directly excited by the laser. This method is very powerful, but it is limited by the frequency range of the IR source (typically  $>1300$   $\text{cm}^{-1}$  for desktop lasers) and limited to energy exchanges faster than molecular rotations. In typical small molecule organic solutions, molecular rotations are generally faster than vibrational energy transfers.

The method introduced here does not observe the modes under energy transfer directly. Instead, it monitors the changes in the “reporters,” which are strongly coupled to the exchanging modes. The exchanging modes can be either resonant or nonresonant. They do not have to be excited by the lasers. They are excited by the energy relaxation of the reporter or other high frequency modes. This will provide the flexibility to choose laser sources. In addition, the method is not limited by the time scale of molecular rotations. It will be particularly useful in the studies of molecular interactions in complicated systems, e.g., antibody/antigen, peptide/DNA, drug/protein interactions, etc., where the vibrational resonance in the frequency range between 500 and 1500  $\text{cm}^{-1}$  is extremely high. Of course, the same strategy can be applied in the IR/Raman method.

There are three main drawbacks in the method introduced here. One is that the details of the exchanging modes are unknown experimentally. Other techniques are required to help identify the modes. Another is that the reporter has to be coupled to the exchanging modes and the combination band between the reporter and the modes needs to be experimentally observable. This is actually less of an issue. Many vibrational modes, e.g., CD, CN, CO, NCO, and CH, have the required properties<sup>16,24,57,84,85</sup> and can serve as the reporter. The last one is that the modes coupled to the reporters have to be on resonance or quasiresonance between two molecules for efficient energy transfers. This will be an issue for simple molecules.

The method is expected to be immediately applicable to detect whether two molecules are close to each. To investigate the molecular details of how they interact requires knowledge about how the coupling strengths, energy mismatches, and molecular distances affect the transfer rate.

#### IV. CONCLUDING REMARKS

The 2D IR method was demonstrated to be able to directly probe intermolecular vibrational energy transfer. In the model system—a benzonitrile and  $\text{CD}_3\text{CN}$  mixture, the CN stretches are first excited to their first excited state. Then within 20 ps, about 20% of the excitations relax to low frequency modes, which exchange their vibrational energy between the two molecules at the time scale of  $\sim 40$  ps. The energy exchange is directly monitored through cross peak growths in 2D IR spectra at the CN 0-1 transition frequency and the combination CN 0-1 absorption frequency. The low frequency modes, which can effectively transfer vibrational energy, are tentatively assigned to be almost the resonant ring breathing motion of benzonitrile and the C–D bending of  $\text{CD}_3\text{CN}$ .

The method can be potentially applied to the studies of molecular interactions in biological systems, e.g., antibody/antigen, peptide/DNA, drug/protein interactions, etc., where the chance of resonance among vibrational modes is big.

#### ACKNOWLEDGMENTS

The nonlinear optical experiments presented in this paper were conducted in the laboratories of Professor Michael D. Fayer, Department of Chemistry, Stanford University. I

would like to thank him and members of his group for their assistance and acknowledge the Air Force Office of Scientific Research (Grant No. F49620-01-1-0018) for support of this work. Other experiments, calculations, and the data analysis were conducted at Rice University. The authors also acknowledge the Welch Foundation and Rice University for support of this work.

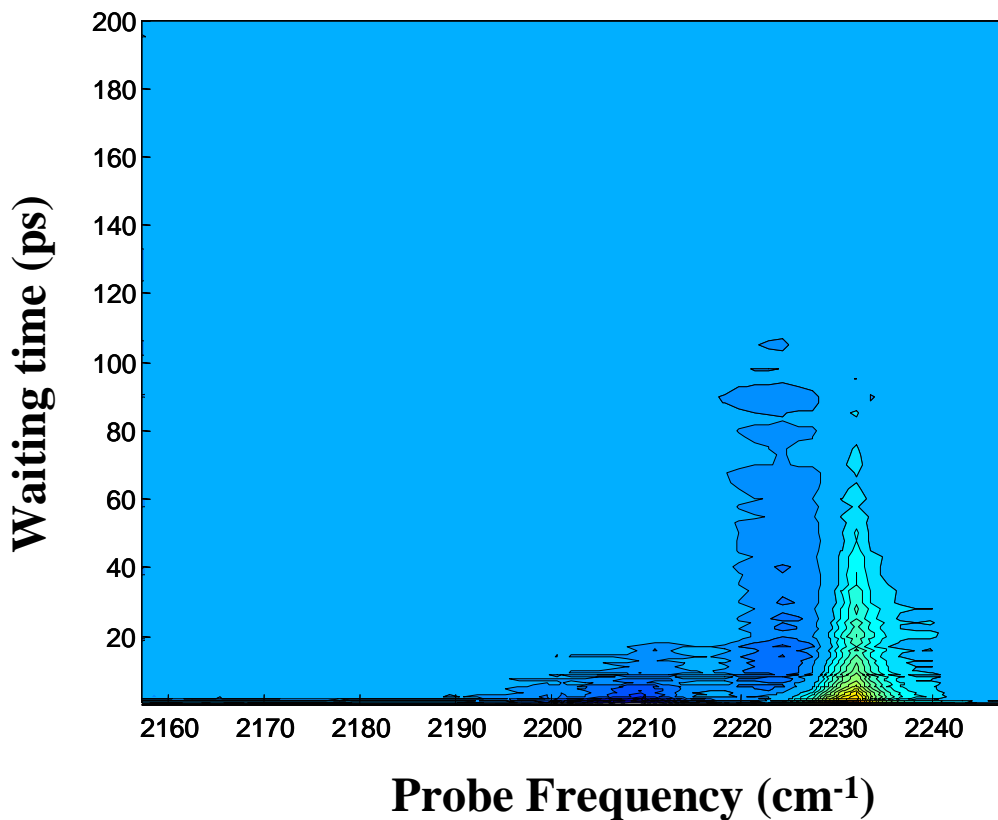
- <sup>1</sup>C. G. Elles and F. F. Crim, *Annu. Rev. Phys. Chem.* **57**, 273 (2006).
- <sup>2</sup>C. B. Harris, D. E. Smith, and D. J. Russell, *Chem. Rev. (Washington, D.C.)* **90**, 481 (1990).
- <sup>3</sup>E. L. Sibert, S. G. Ramesh, and T. S. Gulmen, *J. Phys. Chem. A* **112**, 11291 (2008).
- <sup>4</sup>J. C. Deak, Y. Pang, T. D. Sechler, Z. Wang, and D. D. Dlott, *Science* **306**, 473 (2004).
- <sup>5</sup>D. D. Dlott, *Chem. Phys.* **266**, 149 (2001).
- <sup>6</sup>A. H. Xie, L. van der Meer, W. Hoff, and R. H. Austin, *Phys. Rev. Lett.* **84**, 5435 (2000).
- <sup>7</sup>D. M. Leitner, *Annu. Rev. Phys. Chem.* **59**, 233 (2008).
- <sup>8</sup>Y. Zhang, H. Fujisaki, and J. E. Straub, *J. Phys. Chem. A* **113**, 3051 (2009).
- <sup>9</sup>B. J. Ka and E. Geva, *J. Phys. Chem. A* **110**, 9555 (2006).
- <sup>10</sup>R. Rey, K. B. Moller, and J. T. Hynes, *Chem. Rev. (Washington, D.C.)* **104**, 1915 (2004).
- <sup>11</sup>A. A. Stuchebrukhov and R. A. Marcus, *J. Chem. Phys.* **98**, 8443 (1993).
- <sup>12</sup>D. W. Miller and S. A. Adelman, *Int. Rev. Phys. Chem.* **13**, 359 (1994).
- <sup>13</sup>H. Graener, T. Patzlaff, K. Paradowska-Moszkowska, and G. Seifert, *J. Chem. Phys.* **119**, 8537 (2003).
- <sup>14</sup>V. M. Kenkre, A. Tokmakoff, and M. D. Fayer, *J. Chem. Phys.* **101**, 10618 (1994).
- <sup>15</sup>J. C. Owrtsky, D. Raftery, and R. M. Hochstrasser, *Annu. Rev. Phys. Chem.* **45**, 519 (1994).
- <sup>16</sup>H. J. Bakker, P. C. M. Planken, and A. Lagendijk, *Nature (London)* **347**, 745 (1990).
- <sup>17</sup>S. Woutersen and H. J. Bakker, *Nature (London)* **402**, 507 (1999).
- <sup>18</sup>A. Laubereau and W. Kaiser, *Rev. Mod. Phys.* **50**, 607 (1978).
- <sup>19</sup>R. Laenen, C. Rauscher, and A. Laubereau, *Chem. Phys. Lett.* **283**, 7 (1998).
- <sup>20</sup>A. Laubereau, L. Kirschner, and W. Kaiser, *Opt. Commun.* **9**, 182 (1973).
- <sup>21</sup>L. K. Iwaki and D. D. Dlott, *J. Phys. Chem. A* **104**, 9101 (2000).
- <sup>22</sup>Z. H. Wang, A. Pakoulev, and D. D. Dlott, *Science* **296**, 2201 (2002).
- <sup>23</sup>X. Y. Hong, S. Chen, and D. D. Dlott, *J. Phys. Chem.* **99**, 9102 (1995).
- <sup>24</sup>G. Seifert, R. Zurl, T. Patzlaff, and H. Graener, *J. Chem. Phys.* **112**, 6349 (2000).
- <sup>25</sup>V. Lenchenkov, C. X. She, and T. Q. Lian, *J. Phys. Chem. B* **110**, 19990 (2006).
- <sup>26</sup>P. Hamm, M. Lim, W. F. Degrado, and R. M. Hochstrasser, *J. Chem. Phys.* **112**, 1907 (2000).
- <sup>27</sup>V. Cervetto, J. Helbing, J. Bredenbeck, and P. Hamm, *J. Chem. Phys.* **121**, 5935 (2004).
- <sup>28</sup>S. Woutersen, Y. Mu, G. Stock, and P. Hamm, *Chem. Phys.* **266**, 137 (2001).
- <sup>29</sup>J. Bredenbeck, J. Helbing, and P. Hamm, *J. Am. Chem. Soc.* **126**, 990 (2004).
- <sup>30</sup>J. Bredenbeck, A. Ghosh, M. Smits, and M. Bonn, *J. Am. Chem. Soc.* **130**, 2152 (2008).
- <sup>31</sup>C. Kolano, J. Helbing, M. Kozinski, W. Sander, and P. Hamm, *Nature (London)* **444**, 469 (2006).
- <sup>32</sup>Z. Ganim, H. S. Chung, A. W. Smith, L. P. Deflores, K. C. Jones, and A. Tokmakoff, *Acc. Chem. Res.* **41**, 432 (2008).
- <sup>33</sup>M. Khalil, N. Demirdoven, and A. Tokmakoff, *J. Phys. Chem. A* **107**, 5258 (2003).
- <sup>34</sup>M. Khalil, N. Demirdoven, and A. Tokmakoff, *Phys. Rev. Lett.* **90**, 047401 (2003).
- <sup>35</sup>O. Golonzka, M. Khalil, N. Demirdoven, and A. Tokmakoff, *Phys. Rev. Lett.* **86**, 2154 (2001).
- <sup>36</sup>J. P. Wang, J. X. Chen, and R. M. Hochstrasser, *J. Phys. Chem. B* **110**, 7545 (2006).
- <sup>37</sup>I. V. Rubtsov, K. Kumar, and R. M. Hochstrasser, *Chem. Phys. Lett.* **402**, 439 (2005).
- <sup>38</sup>M. T. Zanni, S. Gnanakaran, J. Stenger, and R. M. Hochstrasser, *J. Phys.*

- Chem. B* **105**, 6520 (2001).
- <sup>39</sup> Y. S. Kim and R. M. Hochstrasser, *Proc. Natl. Acad. Sci. U.S.A.* **102**, 11185 (2005).
- <sup>40</sup> M. C. Asplund, M. T. Zanni, and R. M. Hochstrasser, *Proc. Natl. Acad. Sci. U.S.A.* **97**, 8219 (2000).
- <sup>41</sup> S. Mukamel, *Principles of Nonlinear Optical Spectroscopy* (Oxford University Press, New York, 1995).
- <sup>42</sup> F. Sanda and S. Mukamel, *J. Chem. Phys.* **125**, 014507 (2006).
- <sup>43</sup> Y. Tanimura and S. Mukamel, *J. Chem. Phys.* **99**, 9496 (1993).
- <sup>44</sup> J. F. Cahoon, K. R. Sawyer, J. P. Schlegel, and C. B. Harris, *Science* **319**, 1820 (2008).
- <sup>45</sup> H. Maekawa, F. Formaggio, C. Toniolo, and N. H. Ge, *J. Am. Chem. Soc.* **130**, 6556 (2008).
- <sup>46</sup> S. H. Shim, D. B. Strasfeld, Y. L. Ling, and M. T. Zanni, *Proc. Natl. Acad. Sci. U.S.A.* **104**, 14197 (2007).
- <sup>47</sup> M. L. Cowan, B. D. Bruner, N. Huse, J. R. Dwyer, B. Chugh, E. T. J. Nibbering, T. Elsaesser, and R. J. D. Miller, *Nature (London)* **434**, 199 (2005).
- <sup>48</sup> P. Mukherjee, I. Kass, I. Arkin, and M. T. Zanni, *Proc. Natl. Acad. Sci. U.S.A.* **103**, 3528 (2006).
- <sup>49</sup> H. Maekawa, C. Toniolo, A. Moretto, Q. B. Broxterman, and N. H. Ge, *J. Phys. Chem. B* **110**, 5834 (2006).
- <sup>50</sup> S. R. G. Naraharisetty, V. M. Kasyanenko, and I. V. Rubtsov, *J. Chem. Phys.* **128**, 104502 (2008).
- <sup>51</sup> M. J. Nee, C. R. Baiz, J. M. Anna, R. McCanne, and K. J. Kubarych, *J. Chem. Phys.* **129**, 084503 (2008).
- <sup>52</sup> C. R. Baiz, M. J. Nee, R. McCanne, and K. J. Kubarych, *Opt. Lett.* **33**, 2533 (2008).
- <sup>53</sup> L. W. Barbour, M. Hegadorn, and J. B. Asbury, *J. Am. Chem. Soc.* **129**, 15884 (2007).
- <sup>54</sup> J. B. Asbury, T. Steinel, C. Stromberg, K. J. Gaffney, I. R. Piletic, A. Goun, and M. D. Fayer, *Phys. Rev. Lett.* **91**, 237402 (2003).
- <sup>55</sup> J. Zheng, K. Kwak, and M. D. Fayer, *Acc. Chem. Res.* **40**, 75 (2007).
- <sup>56</sup> J. R. Zheng and M. D. Fayer, *J. Am. Chem. Soc.* **129**, 4328 (2007).
- <sup>57</sup> J. Zheng, K. Kwac, J. Xie, and M. D. Fayer, *Science* **313**, 1951 (2006).
- <sup>58</sup> J. Zheng, K. Kwak, J. B. Asbury, X. Chen, I. Piletic, and M. D. Fayer, *Science* **309**, 1338 (2005).
- <sup>59</sup> V. Cervetto, P. Hamm, and J. Helbing, *J. Phys. Chem. B* **112**, 8398 (2008).
- <sup>60</sup> M. Kozinski, S. Garrett-Roe, and P. Hamm, *J. Phys. Chem. B* **112**, 7645 (2008).
- <sup>61</sup> I. J. Finkelstein, J. R. Zheng, H. Ishikawa, S. Kim, K. Kwak, and M. D. Fayer, *Phys. Chem. Chem. Phys.* **9**, 1533 (2007).
- <sup>62</sup> I. J. Finkelstein, H. Ishikawa, S. Kim, A. M. Massari, and M. D. Fayer, *Proc. Natl. Acad. Sci. U.S.A.* **104**, 2637 (2007).
- <sup>63</sup> J. Treuffet, K. J. Kubarych, J. C. Lambry, E. Pilet, J. B. Masson, J. L. Martin, M. H. Vos, M. Joffre, and A. Alexandrou, *Proc. Natl. Acad. Sci. U.S.A.* **104**, 15705 (2007).
- <sup>64</sup> H. Ishikawa, K. Kwak, J. K. Chung, S. Kim, and M. D. Fayer, *Proc. Natl. Acad. Sci. U.S.A.* **105**, 8619 (2008).
- <sup>65</sup> M. F. DeCamp, L. DeFlores, J. M. McCracken, A. Tokmakoff, K. Kwac, and M. Cho, *J. Phys. Chem. B* **109**, 11016 (2005).
- <sup>66</sup> C. Fang, J. D. Bauman, K. Das, A. Remorino, E. Arnold, and R. M. Hochstrasser, *Proc. Natl. Acad. Sci. U.S.A.* **105**, 1472 (2008).
- <sup>67</sup> P. Mukherjee, I. Kass, I. T. Arkin, and M. T. Zanni, *J. Phys. Chem. B* **110**, 24740 (2006).
- <sup>68</sup> L. W. Barbour, M. Hegadorn, and J. B. Asbury, *J. Phys. Chem. B* **110**, 24281 (2006).
- <sup>69</sup> M. Khalil, N. Demirdoven, and A. Tokmakoff, *J. Chem. Phys.* **121**, 362 (2004).
- <sup>70</sup> J. Zheng, K. Kwak, T. Steinel, J. B. Asbury, X. Chen, J. Xie, and M. D. Fayer, *J. Chem. Phys.* **123**, 164301 (2005).
- <sup>71</sup> S. R. G. Naraharisetty, D. V. Kurochkin, and I. V. Rubtsov, *Chem. Phys. Lett.* **437**, 262 (2007).
- <sup>72</sup> D. E. Moilanen, D. Wong, D. E. Rosenfeld, E. E. Fenn, and M. D. Fayer, *Proc. Natl. Acad. Sci. U.S.A.* **106**, 375 (2009).
- <sup>73</sup> J. B. Asbury, T. Steinel, C. Stromberg, S. A. Corcelli, C. P. Lawrence, J. L. Skinner, and M. D. Fayer, *J. Phys. Chem. A* **108**, 1107 (2004).
- <sup>74</sup> T. Steinel, J. B. Asbury, S. A. Corcelli, C. P. Lawrence, J. L. Skinner, and M. D. Fayer, *Chem. Phys. Lett.* **386**, 295 (2004).
- <sup>75</sup> J. J. Loparo, S. T. Roberts, R. A. Nicodemus, and A. Tokmakoff, *Chem. Phys.* **341**, 218 (2007).
- <sup>76</sup> J. J. Loparo, S. T. Roberts, and A. Tokmakoff, *J. Chem. Phys.* **125**, 12 (2006).
- <sup>77</sup> C. J. Fecko, J. D. Eaves, J. J. Loparo, A. Tokmakoff, and P. L. Geissler, *Science* **301**, 1698 (2003).
- <sup>78</sup> J. Zheng, K. Kwak, X. Chen, J. B. Asbury, and M. D. Fayer, *J. Am. Chem. Soc.* **128**, 2977 (2006).
- <sup>79</sup> J. Zheng and M. D. Fayer, *J. Phys. Chem. B* **112**, 10221 (2008).
- <sup>80</sup> J. B. Asbury, T. Steinel, and M. D. Fayer, *J. Lumin.* **107**, 271 (2004).
- <sup>81</sup> R. G. Parr and W. Yang, *Density Functional Theory of Atoms and Molecules* (Oxford University Press, New York, 1989).
- <sup>82</sup> Y. R. Shen, *The Principles of Nonlinear Optics* (Wiley, New York, 1984).
- <sup>83</sup> See EPAPS supplementary material at <http://dx.doi.org/10.1063/1.3212618> for more experimental and calculation information.
- <sup>84</sup> D. V. Kurochkin, S. R. G. Naraharisetty, and I. V. Rubtsov, *Proc. Natl. Acad. Sci. U.S.A.* **104**, 14209 (2007).
- <sup>85</sup> J. R. Zheng, Stanford University, 2007.
- <sup>86</sup> J. C. Deak, L. K. Iwaki, and D. D. Klott, *J. Phys. Chem. A* **102**, 8193 (1998).
- <sup>87</sup> M. Katayama, K. Komori, K. Ozutsumi, and H. Ohtaki, *Zeitschrift Fur Physikalische Chemie-International Journal of Research in Physical Chemistry & Chemical Physics* **218**, 659 (2004).
- <sup>88</sup> T. Steinel, J. B. Asbury, J. R. Zheng, and M. D. Fayer, *J. Phys. Chem. A* **108**, 10957 (2004).
- <sup>89</sup> J. B. Asbury, T. Steinel, and M. D. Fayer, *J. Phys. Chem. B* **108**, 6544 (2004).

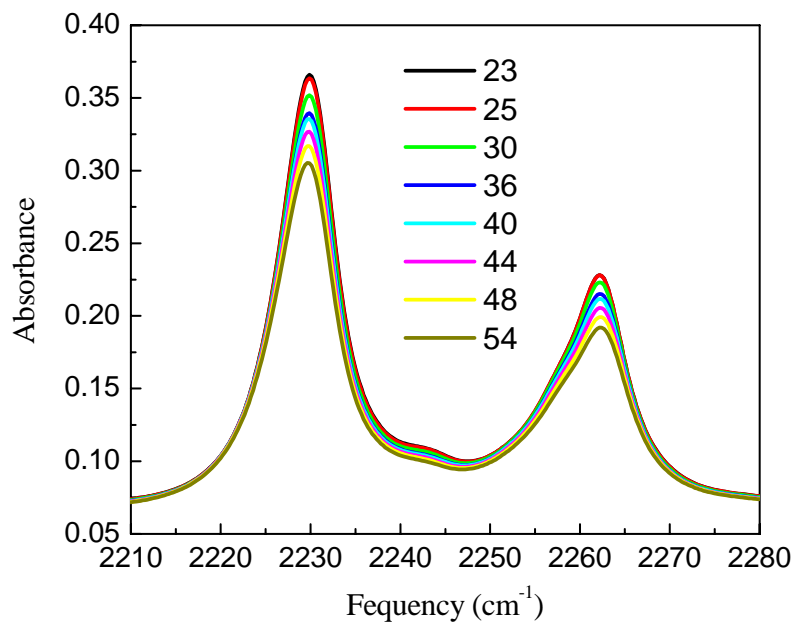
# Intermolecular Vibrational Energy Exchange Directly Probed with Ultrafast Two Dimensional Infrared Spectroscopy

*Hongtao Bian, Wei Zhao, and Junrong Zheng*

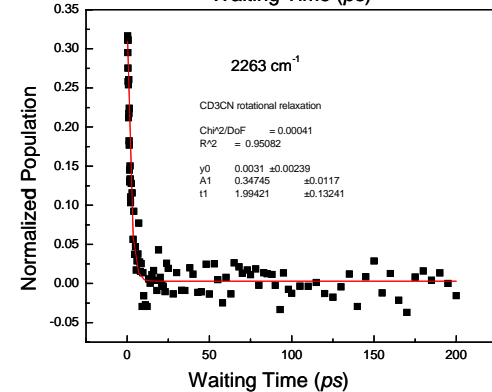
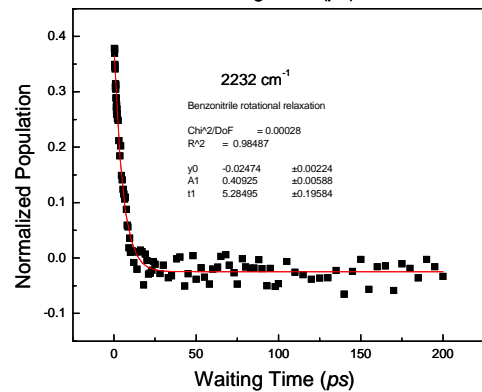
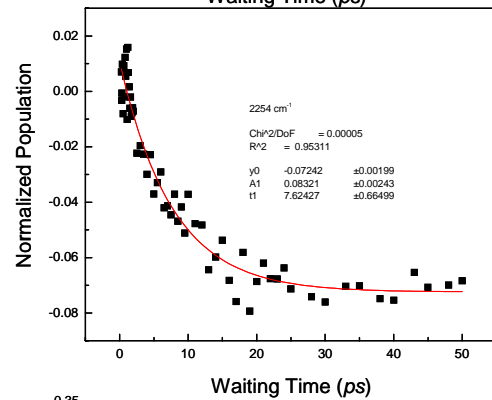
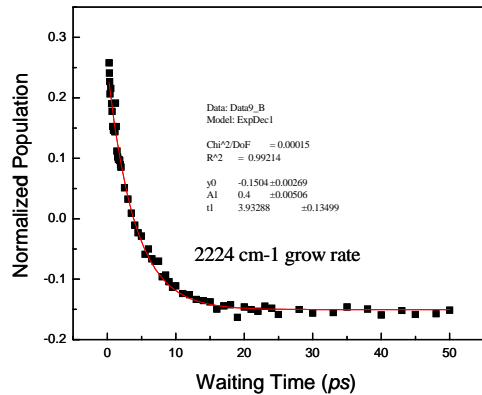
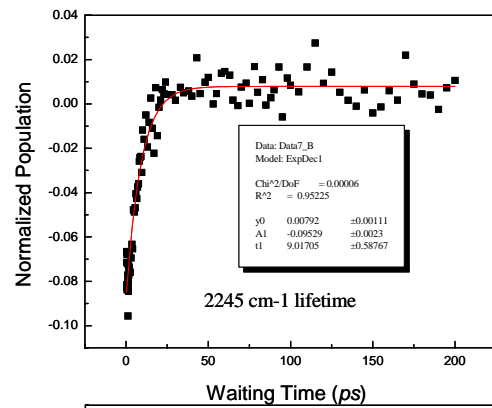
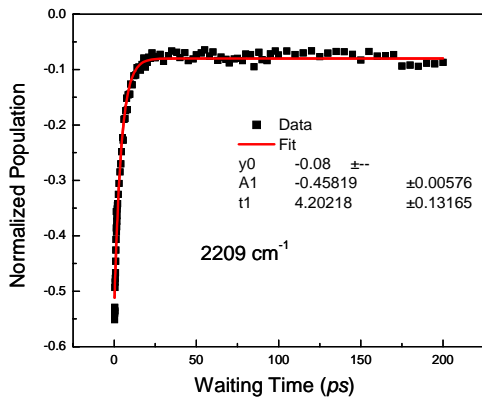
## Supporting materials



**S1.** Rotation-free pump/probe data of 1.8 wt% benzonitrile in CCl<sub>4</sub> at room temperature. One contour represents 4% of the intensity. The peak intensity ratio of the red/blue at long delay times shows the cross section ratio between the combination band and the CN 0-1 transition. In the dilute solution, heat effect is negligible. In the mixed sample, the heat effect is not negligible. The ratio determined here can be used to determine the ratio of the contribution of L' or L over that of heat to the red peaks in 2D IR spectra in panel 30ps in fig.1.

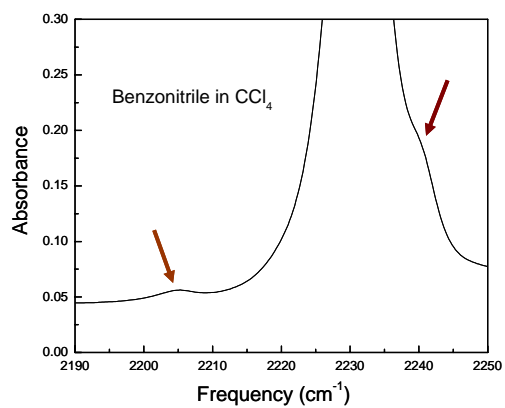
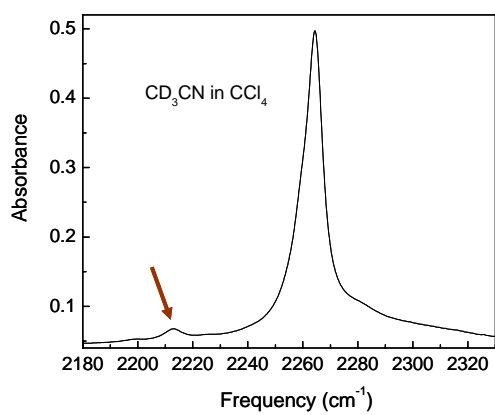


**S2.** Temperature dependent FTIR spectra of CD<sub>3</sub>CN and Benzonitrile mixture. The temperature increase reduces the cross sections of both CN absorptions.

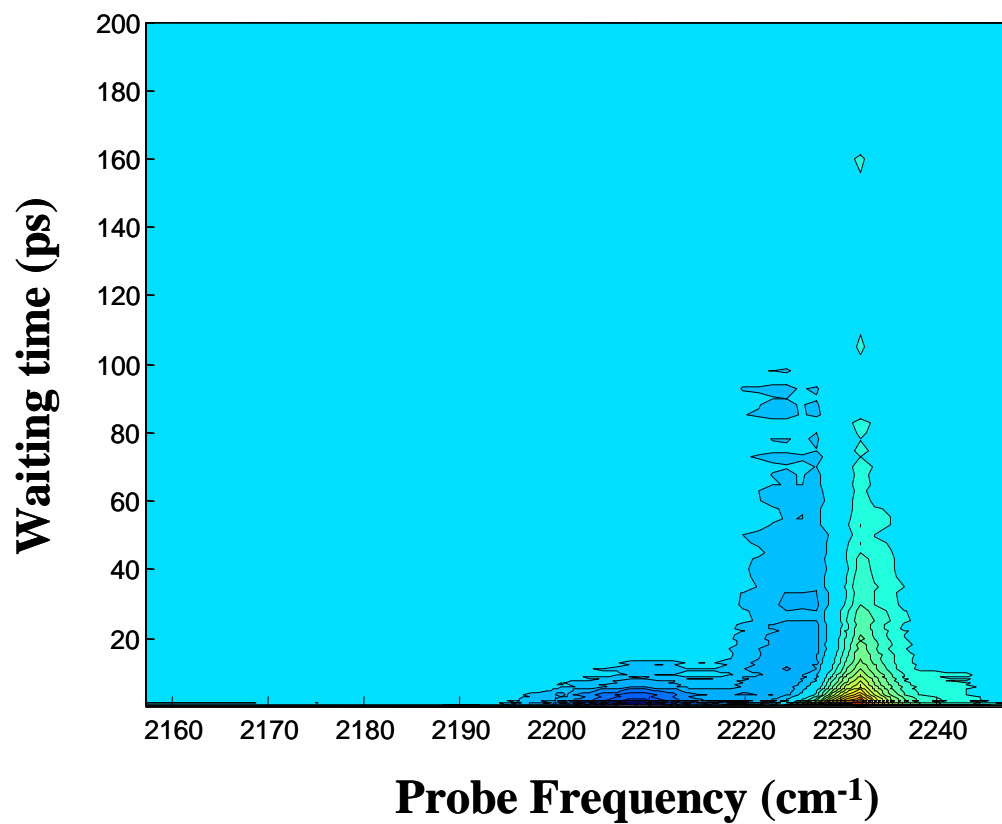


### S3. Pump/probe data and fits to obtain the time constants

CN vibrational lifetimes are from single exponential fits to the pp signals at the CN 1-2 transition frequencies 2245 and 2209  $\text{cm}^{-1}$ , yielding  $T_A = 9 \text{ ps}$ ,  $T_B = 4.2 \text{ ps}$ . The relaxation time constants to L and L' are obtained from fitting pp data at the combination band absorption frequencies 2254 and 2224  $\text{cm}^{-1}$  at delay shorter than 50ps, yielding  $T_{AL} = 7.6 \text{ ps}$ ,  $T_B = 3.9 \text{ ps}$ , since the combination band signal is from the excitation of L or L'. The lifetimes of L and L' are obtained from the decays of the pp data at the combination band absorption frequencies 2254 and 2224  $\text{cm}^{-1}$  at delay between 50 to 200ps. The energy ratio deposit into A and B and the transition dipole moment ratio are determined from the IR absorption peak area ratio based on the Lambert Beer Law.



**S4.** FTIR spectra of  $\text{CD}_3\text{CN}$  and Benzonitrile in  $\text{CCl}_4$  showing the origins of small peaks in pump/probe data and 2D IR data



**S5.** Rotation-free pump/probe data of 2.5 wt% benzonitrile in chloroform at room temperature. One contour represents 4% of the intensity.

## Temperature Increase Estimation

The pump/probe signal difference between 20ps and 200ps delays experimentally obtained is

$$\left(\frac{T_{200}}{T_r} - \frac{T_{np}}{T_r}\right) / \left(\frac{T_{np}}{T_r}\right) - \left(\frac{T_{20}}{T_r} - \frac{T_{np}}{T_r}\right) / \left(\frac{T_{np}}{T_r}\right) = (T_{200} - T_{20}) / T_{np} ,$$

where  $T_{200}$ , and  $T_{20}$  are the light intensities transmitting through the sample at delay 200ps and 20ps, respectively.  $T_r$  is the reference intensity, and  $T_{np}$  is the intensity before pump.

The pump excites about 2% population initially. According to the Beer-Lambert Law, the transmittance–pp signal changes about 2.3%, caused by the population change. Now take the benzonitrile as an example. The signal at 200ps is ~26% of the initial one, while at 20ps, it is about 18%. These give the pp signal to be  $0.023 * (0.26 - 0.18) = 0.18\%$ . Energy exchanges cause the signal ~8% of initial population smaller, resulting in total 0.36% bleaching by heating. In the temperature dependent IR measurements, the transmittance change between 25<sup>o</sup>C to 30<sup>o</sup>C is ~0.02. If we assume the change with temperature is linear, then the pp signal difference between 200ps and 20ps is ~1K. The temperature measurements and the excited population estimations are not very precise. The estimated uncertainty would be 0.5~2K. The value estimated here is quite consistent with Dlott et al's work<sup>1</sup>.

- (1) Deak, J. C.; Iwaki, L. K.; Dlott, D. D. *Journal of Physical Chemistry A* **1998**, *102*, 8193-8201.